Electronic Supplementary Material (ESI) for Materials Advances.

Detection of Al^{3+} and Cu^{2+} ions by isonicotinohydrazide based chemosensors and its application to live cell imaging.

In-ho Song [b†], Pritam Torawane[a†], Jung-Seop Lee[b], Shrikant Dashrath Warkad[d], Amulrao Borase[a], Suban K. Sahoo[c] and Satish Balasaheb Nimse[b*], Anil Kuwar[a*]

[a]School of Chemical Sciences, KBC-North Maharashtra University, Jalgaon 425001, India
[b]Institute of Applied Chemistry and Department of Chemistry, Hallym University, Chuncheon 200702, Republic of Korea
[c]Department of Applied Chemistry, SV National Institute of Technology, Surat 395007, Gujrat, India
[d]Biometrix Technology, Inc., 2-2 Bio Venture Plaza 56, Chuncheon 24232, Korea
[*]Corresponding authors: kuwaras@gmail.com (AK); satish_nimse@hallym.ac.kr (SBN)
[†]These authors contributed equally. Hence, both should be considered as first authors.

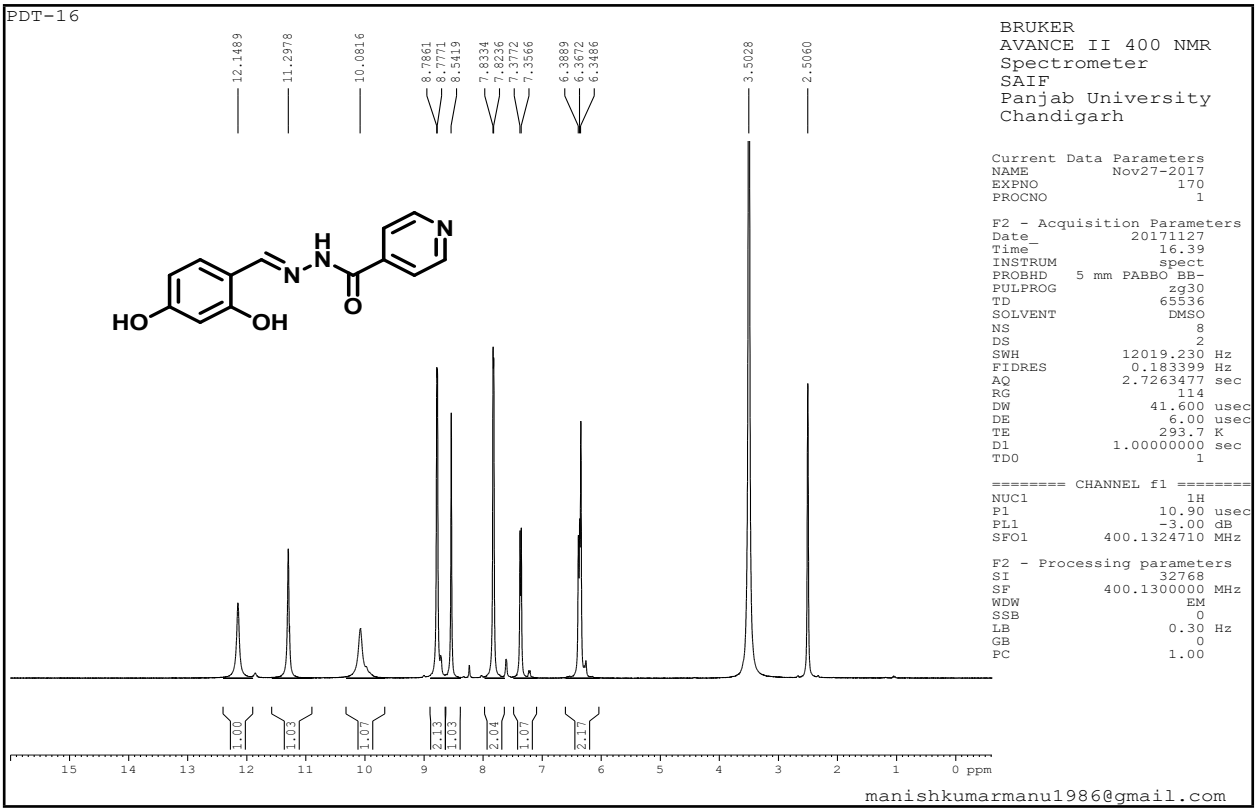

Figure S1.[1]H-NMR spectrum of receptor **3**.

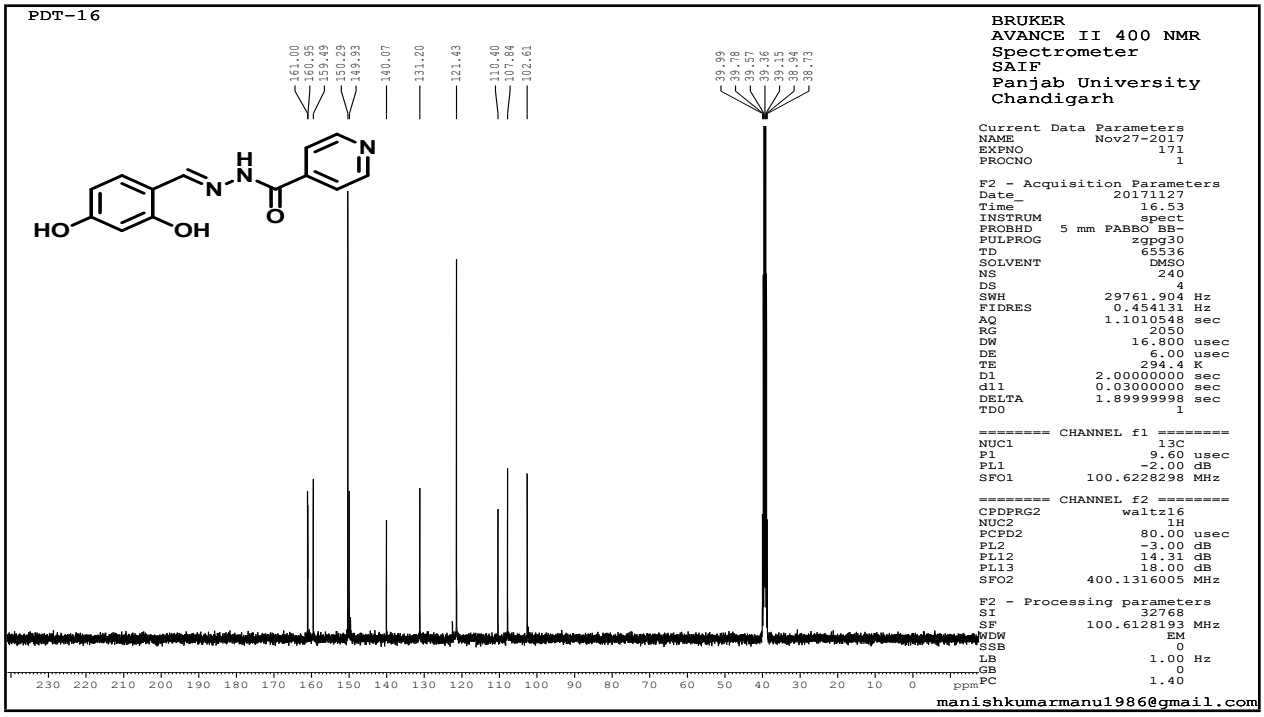

Figure S2. [13]C NMR spectrum of receptor **3**.

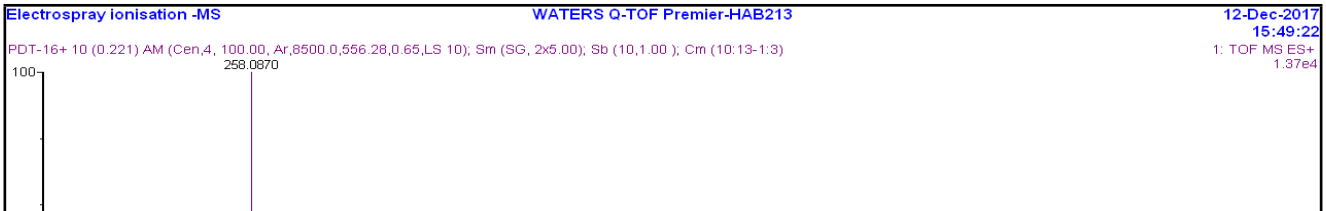

Figure S3. Mass spectrum of receptor **3**.

Table S1. Crystal data, data collection, and structure refinement details for receptor **3**.

Crystal data	Receptor **3**
Formula	$C_{13}H_{11}N_3O_3$
Formula mass (g/mol)	257.25
Crystal system	Orthorhombic
Space group	*Pna*2$_1$
a, b, c (Å)	27.633 (7), 5.5391 (12), 7.6322 (5)
α, β, γ (°)	90, 90, 90
V (Å^3); Z	1168.2 (4); 4
Temperature (K)	150
Radiation type	MoKα (λ = 0.71073)
μ (mm^{-1})	0.11
Collected reflections	22746
2Θ range (°)	5.9, 66.4
Unique reflections	4006
Goodness-of-fit (GOF) on F^2	1.038
R_{int}	0.0652
R_{sigma}	0.0394
R_1 [I≥2σ (I)]	0.0343
wR_2	0.0859
F(000)	536.0
Crystal size (mm)	0.550 × 0.420 × 0.050
Crystal description	Needle, orange
CCDC	CCDC 2051947

Table S2. Selected bond lengths (Å) and bond angles (°) for receptor **3**.

Bond lengths (Å)				**Bond Angles (°)**			
O1—C3	1.3562 (17)	C6—C7	1.381 (2)	C3—O1—H1A	106.5 (16)	O2—C5—C4	117.88 (13)
O1—H1	0.81 (2)	C8—C9	1.500 (2)	C5—O2—H2A	107.7 (16)	O2—C5—C6	121.53 (13)
O2—C5	1.3521 (17)	C9—C10	1.389 (2)	C1—N1—N2	114.70 (12)	C4—C5—C6	120.59 (13)
O2—H2	0.84 (3)	C9—C13	1.394 (2)	C8—N2—N1	119.47 (12)	C7—C6—C5	118.84 (14)
O3—C8	1.2318 (17)	C10—C11	1.384 (2)	C8—N2—H2	123.3 (12)	C6—C7—C2	122.00 (13)
N1—C1	1.2899 (19)	C12—C13	1.389 (2)	N1—N2—H2	117.2 (12)	O3—C8—N2	123.89 (14)
N1—N2	1.3917 (17)	C4—C5	1.389 (2)	C12—N3—C11	117.70 (13)	O3—C8—C9	120.90 (13)
N2—C8	1.3447 (19)			N1—C1—C2	121.68 (13)	N2—C8—C9	115.19 (12)
N2—H2	0.90 (2)			C3—O1—H1A	106.5 (16)	C10—C9—C13	118.37 (13)
N3—C12	1.3391 (19)			C5—O2—H2A	107.7 (16)	C10—C9—C8	117.95 (12)
N3—C11	1.340 (2)			C7—C2—C3	118.31 (13)	C13—C9—C8	123.67 (13)
C1—C2	1.4430 (19)			C7—C2—C1	118.94 (13)	C11—C10—C9	119.01 (13)
C2—C7	1.400 (2)			C3—C2—C1	122.75 (13)	N3—C11—C10	123.13 (13)
C2—C3	1.4151 (19)			O1—C3—C4	118.10 (13)	N3—C12—C13	123.19 (14)
C3—C4	1.394 (2)			O1—C3—C2	121.73 (12)	C12—C13—C9	118.58 (13)
C4—C5	1.389 (2)			C4—C3—C2	120.17 (13)		
C5—C6	1.406 (2)			C5—C4—C3	120.07 (13)		

Table S3. Selected hydrogen-bond lengths (Å) and hydrogen-bond angles (°) for receptor **3**.

D—H···A	D—H (Å)	H···A (Å)	D···A (Å)	D—H···A (°)
O1—H1A···N1	0.81 (2)	1.92 (3)	2.6532 (17)	150 (2)
O2—H2A···N3^{i}	0.84 (3)	1.93 (3)	2.7542 (18)	167 (3)
N2—H2···O3^{ii}	0.90 (2)	1.96 (2)	2.8418 (17)	167.0 (18)
C1—H1···O3^{ii}	0.95	2.49	3.2553 (19)	137.9
C13—H13···O3^{ii}	0.95	2.57	3.327 (2)	136.3

Symmetry code(s): (i) *x*+1/2, -*y*+1/2, *z*; (ii) -*x*+3/2, *y*-1/2, *z*-1/2.

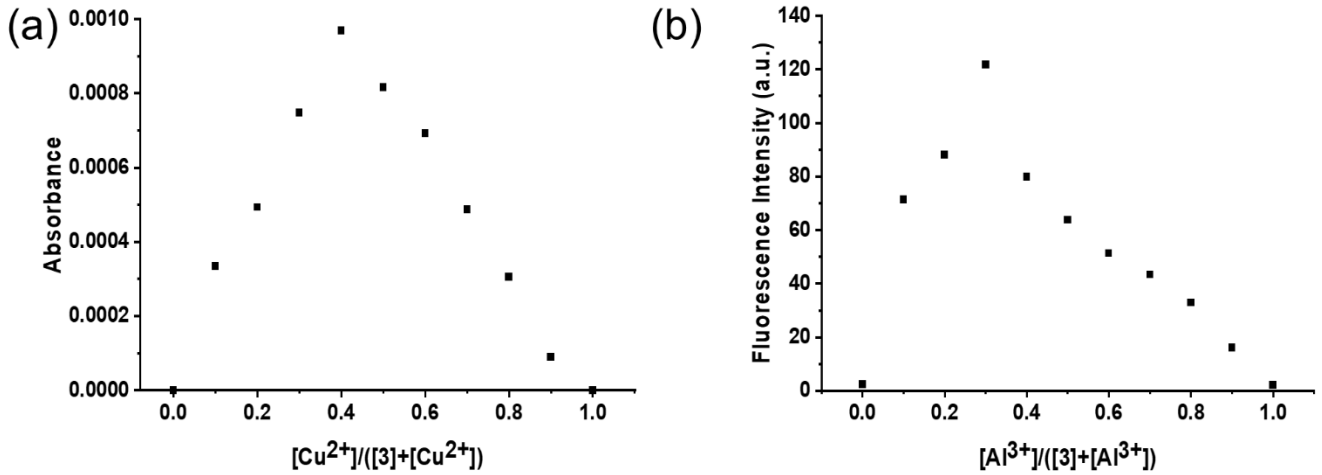

Figure S4. Job's plot of 2:1 binding stoichiometry (a) between receptor **3** and Cu^{2+} ion by UV-visible absorption spectroscopy (λ = 343 nm) and (b) between receptor **3** and Al^{3+} ion by fluorescence spectroscopy (λ_{ex} = 343 nm, λ_{em} = 473 nm).

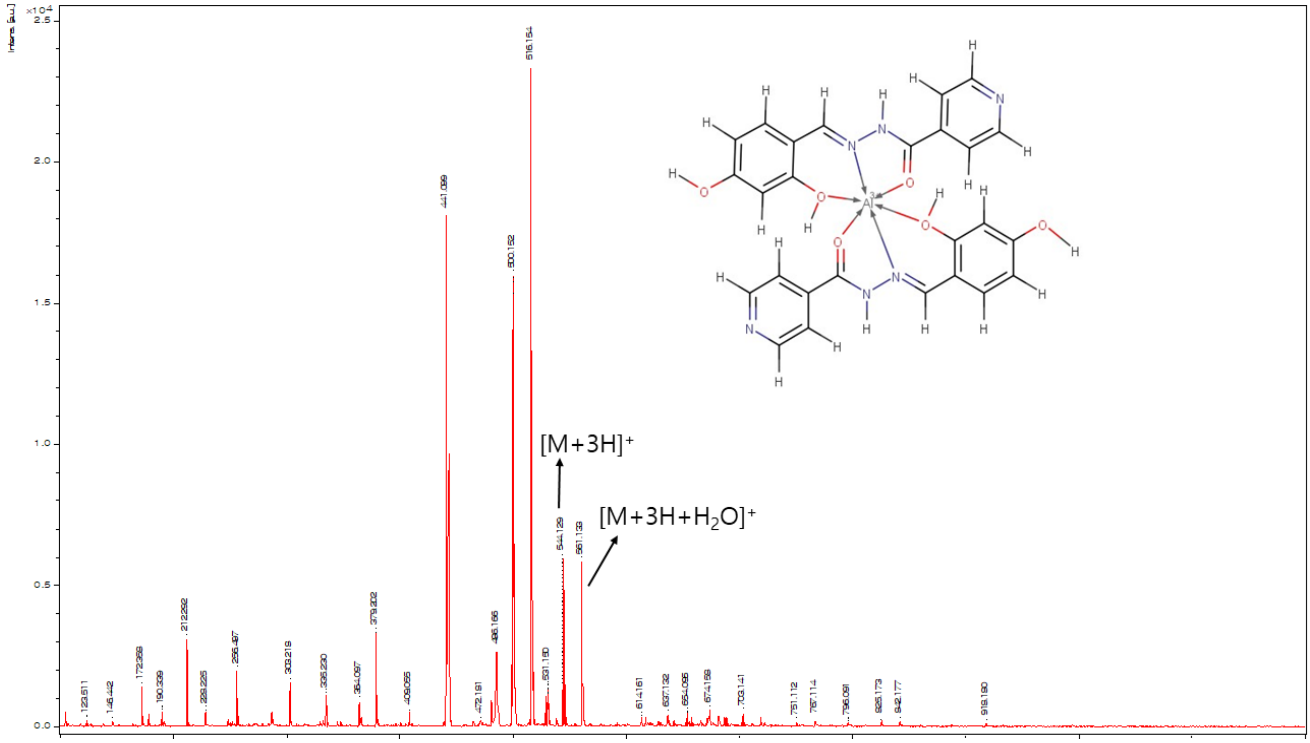

Figure S5. HR-Mass spectrum of the 2:1 (**3.Al^{3+}**) complex

Benesi-Hildebrand equations

$$\frac{1}{(A - A_0)} = \frac{1}{K^{0.5}(A_{max} - A_0)[Cu^{2+}]^{0.5}} + \frac{1}{(A_{max} - A_0)} \qquad (Eq.\,S1)$$

Where,

A_0 is the absorbance of receptor **4** (λ = 400 nm)

A is the observed absorbance in the presence of the varying [Cu^{2+}]

A_{max} is the maximum absorbance obtained at λ= 400 nm during the titration with [Cu^{2+}]

K_a is the association constant (M^{-1})

[Cu^{2+}] is the concentration of the Cu^{2+} ion added during titration studies.

$$\frac{1}{(F - F_0)} = \frac{1}{K^{0.5}(F_{max} - F_0)[Al^{3+}]^{0.5}} + \frac{1}{(F_{max} - F_0)} \qquad (Eq.\,S2)$$

Where,

I_0 is the fluorescence intensity of free receptor **4**,

I, is the observed fluorescence intensity in the presence of the varying [Al^{3+}]

I_{max} is the maximum observed fluorescence intensity (λex = 340 nm, λem= 473 nm) up on titration with [Al^{3+}]

K_a is the association constant (M^{-1})

[Al^{3+}] is the concentration of the Al^{3+} ion added during titration studies.

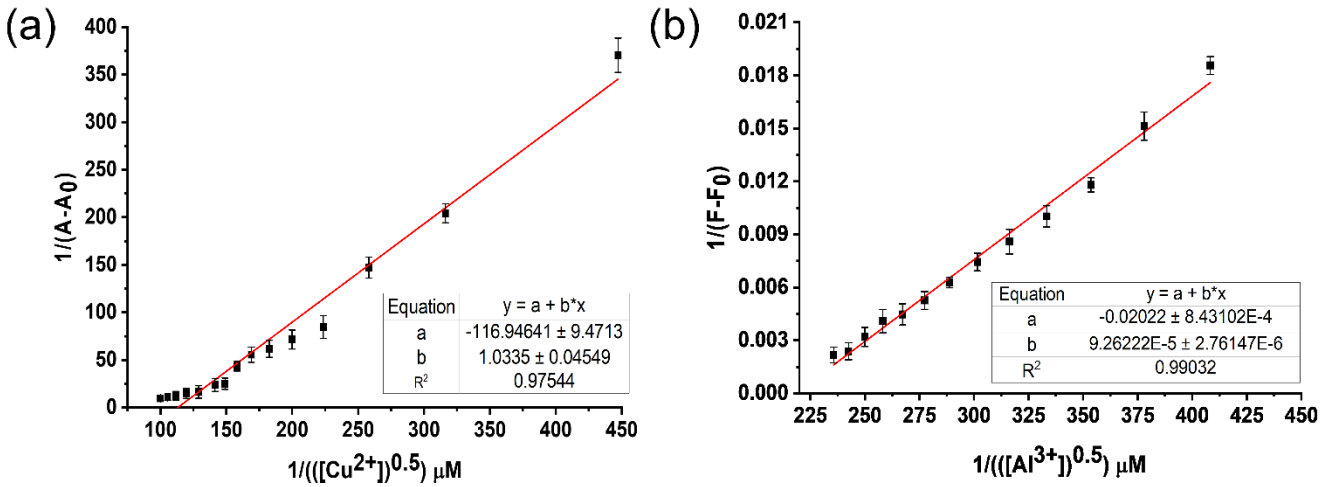

Figure S6. Benesi-Hildebrand Plot of receptor **3** upon titration with (a) Cu^{2+} ions using absorbance values (λ = 413 nm) and (b) Al^{3+} ions using fluorescence emission values (λex = 343 nm, λem = 473 nm).

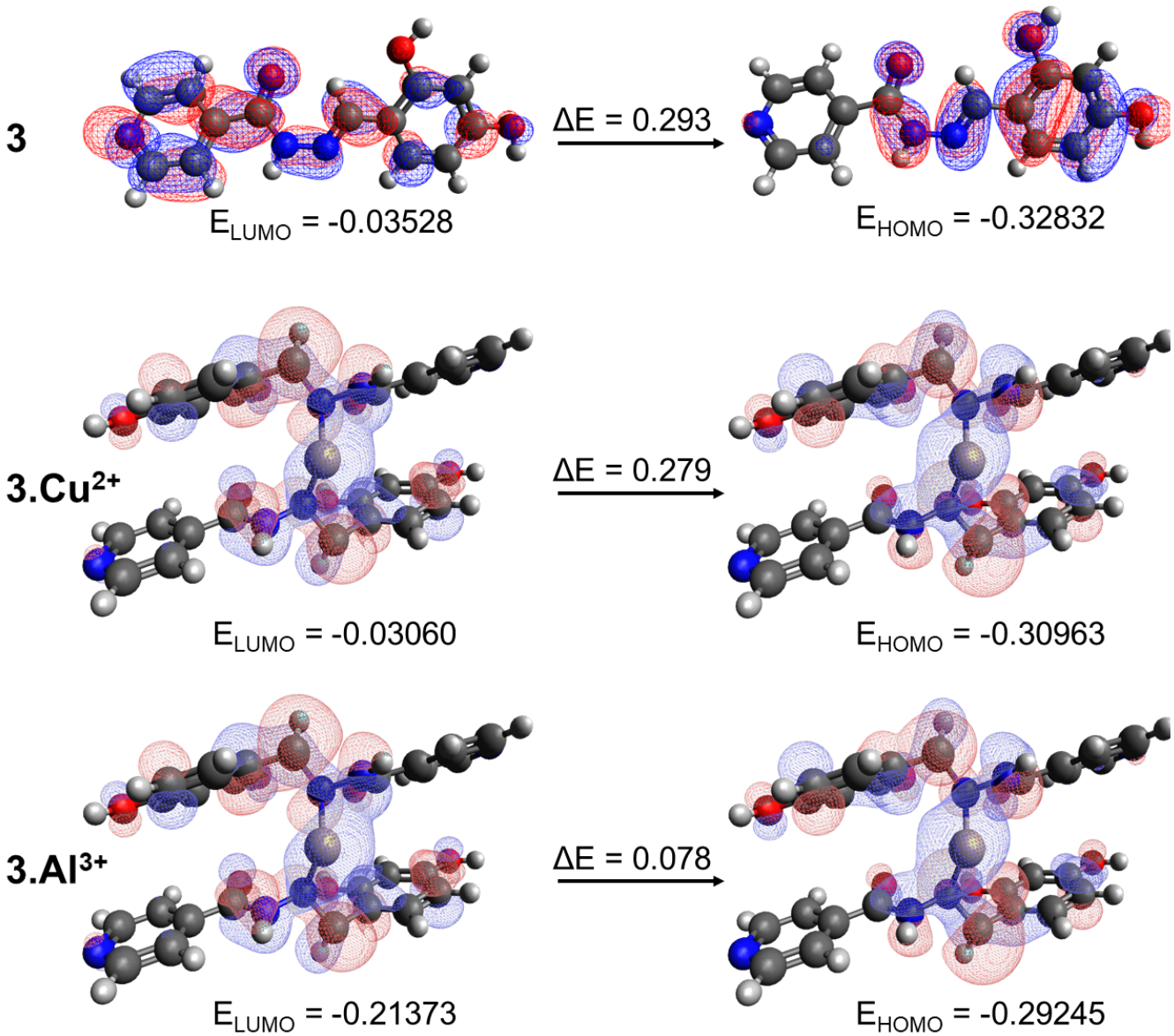

Figure S7. DFT optimized structures of receptor **3** and its **3.Cu**$^{2+}$ and **3.Al**$^{3+}$ complexes by hybrid B3LYP functions with a 6-31G++(d,p) and LANL2DZ basis sets. The LUMO's and HOMO's are illustrated with respective energies.

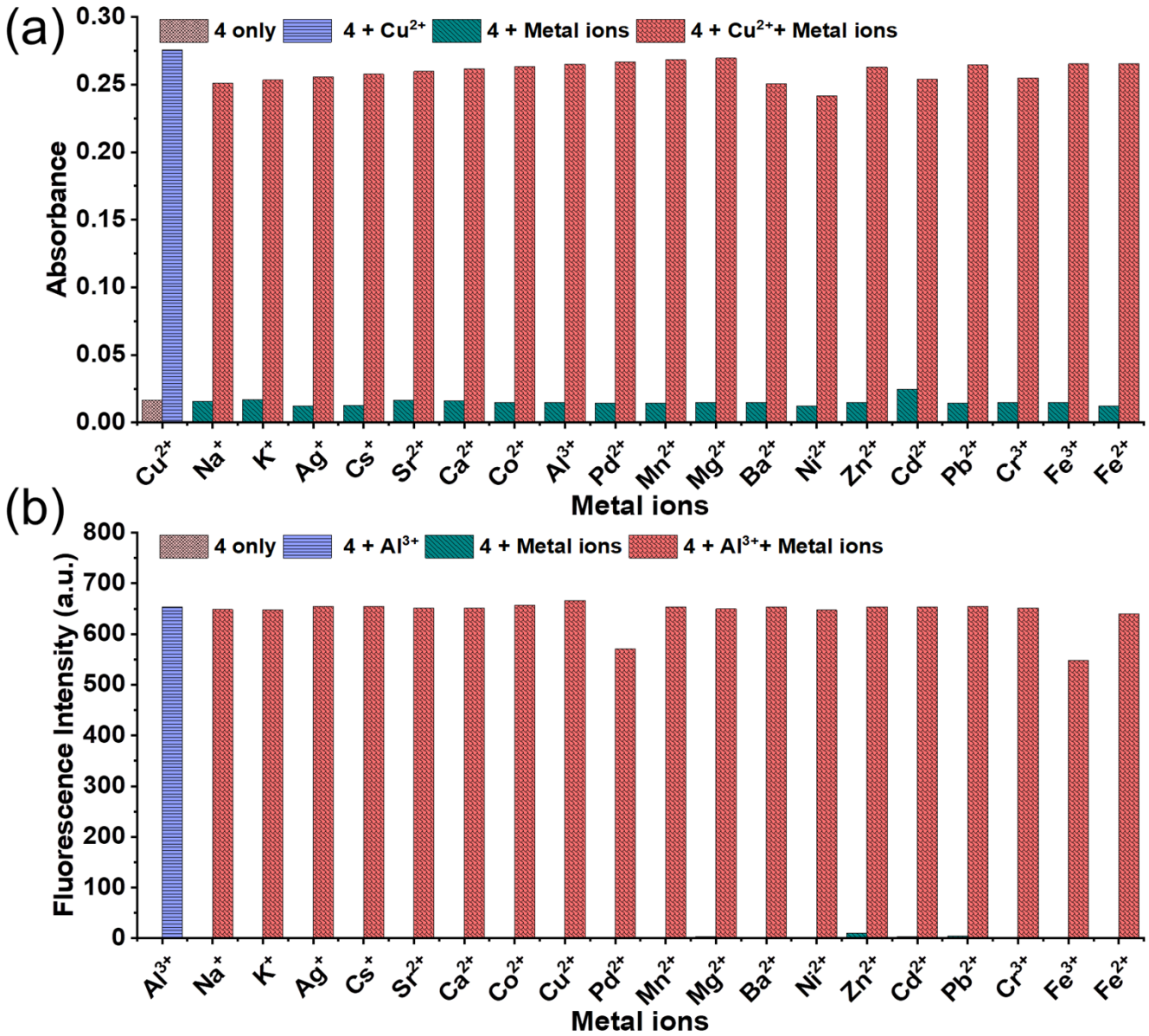

Figure S8. Competitive study of receptor **3** (a) with Cu^{2+} by UV–vis absorption spectroscopy (λ = 413 nm) and (b) with Al^{3+} by fluorescence spectroscopy (λex = 343 nm, λem = 473 nm) in the absence and presence of four equivalents of other metals ions.

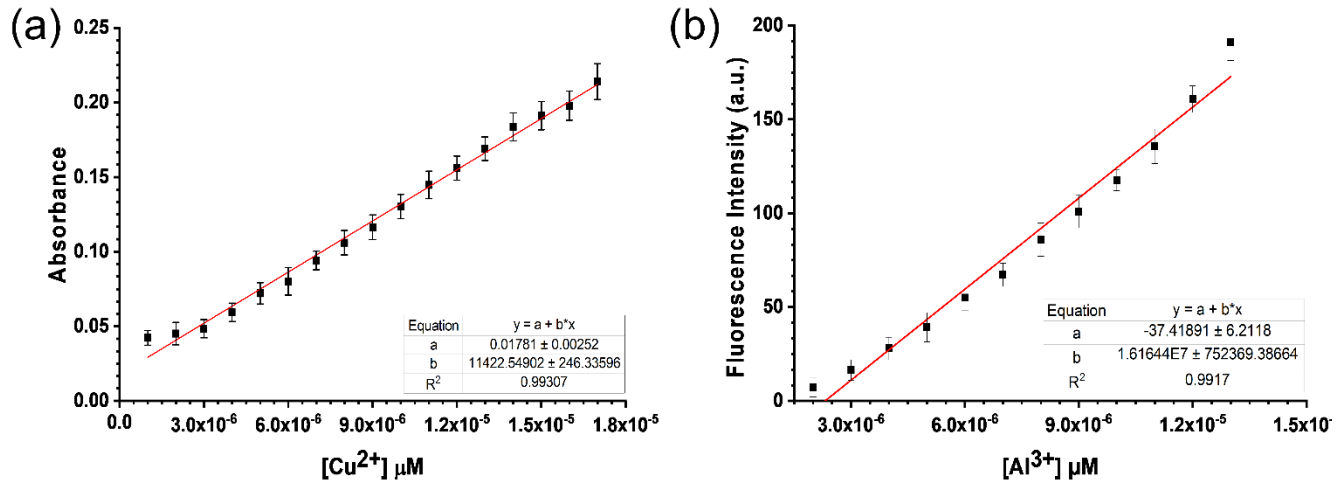

Figure S9. Calibration curves for the detection of (a) Cu^{2+} by UV–vis absorption spectroscopy (λ = 413 nm) and (b) Al^{3+} by fluorescence spectroscopy (λ_{ex} = 343 nm, λ_{em} = 473 nm).

Table S4: Comparison of Cu^{2+} detection limits by present work and reported methods

Group	Detection limit	Response	Ref.
Kim et al.	2.9 μM	Fluorescence	1
Singh et al.	30 μM	Fluorescence	2
Chawla et al.	6 μM	Fluorescence	3
Maity et al.	20 μM	UV, Fluorescence	4
Singh et al.	35 μM-10 nM	Fluorescence	5
Kuwar et al.	**1.9 μM**	**UV- Visible**	**Present Work**

Table S5: Comparison of Al^{3+} detection limits by present work and reported methods

Group	Detection limit	Response	Ref.
Kuwar et al.	0.42 μM	Fluorescence	6
Kuwar et al.	99.5 nM	Fluorescence	7
Tang et al.	3.60 μM	Fluorescence	8
Saha et al.	6.93 nM	Fluorescence	9
Kuwar et al.	**3.0 nM**	Fluorescence	**Present Work**

References:

1. G. J. Park, G. R. You, Y. W. Choi, C. Kim, *Sensors and Actuators B: Chemical*, **2016**, *229*, 257.
2. P. Kaur, D. Sareen, K. Singh, *Talanta*, **2011**, *83*, 1695-1700.
3. H.M. Chawla, P. Goel, R. Shukla, Tetrahedron Letters, **2013**, *54*, 2766–2769.
4. D. Maity, A. K. Manna, D. Karthigeyan, T. K. Kundu, S. K. Pati, T. Govindaraju, *Chem. Eur. J.,* **2017**, *17*, 11152-11161.
5. A.Singh, Q. Yao, L. Tong, W. C. Still, D. Sames, *Tetrahedron Lett.*, **2000**, *41*, 9601-9605.
6. R Patil, A Moirangthem, R Butcher, N Singh, A Basu, K Tayade, U Fegade, A. Kuwar, *Dalton Transactions*, **2014**, *43 (7)*, 2895-2899.
7. P. Torawane, K. Tayade, S. Bothra, S. K. Sahoo, N. Singh, A. Borse, A. Kuwar, *Sensors and Actuators B: Chemical*, **2016**, *222*, 562-566.
8. C. Gao, P. Zang, W. Liu Y. Tang, *J. Fluorescence,* **2016**, *26*, 2015-2021.
9. S. Banerjee, P. Brandão, and A. Saha, *RSC Adv.*, **2016**, *6*, 101924-101936.